RSC Advances

ROYAL SOCIETY OF CHEMISTRY

www.rsc.org/advances

Journal Name

ARTICLE

Photocatalytic conversion of glucose in aqueous suspensions of heteropolyacid-TiO_2 composites

Received 00th January 20xx,
Accepted 00th January 20xx

DOI: 10.1039/x0xx00000x

www.rsc.org/

M. Bellardita[a], E. I. García-López[a]*, G. Marcì[a], B. Megna[b], F. R. Pomilla[a] and L. Palmisano[a]

Commercial and home prepared TiO_2 samples were functionalized with a commercial Keggin heteropolyacid (HPA) $H_3PW_{12}O_{40}$ (PW_{12}) or with a hydrothermally home prepared $K_7PW_{11}O_{39}$ salt (PW_{11}). All the materials were characterized by specific surface area measurements (BET), XRD analyses, Raman, DRS along with SEM observations and they have been used for glucose photocatalytic conversion in aqueous suspension. Different reaction extent and distribution of intermediate oxidation products were observed depending on the photocatalyst. Gluconic acid, arabinose, erythrose and formic acid were observed as oxidation products when bare TiO_2 or HPA/TiO_2 composite materials were used. Glucose isomerization to form fructose was also observed and in some runs traces of glucaric acid and glyceraldehyde were also found. The carbon mass balance was accomplished in the presence of the commercial Evonik P25 TiO_2 powder and the composites where TiO_2 was present, whereas the presence of the solvothermically prepared TiO_2 gave rise to a carbon unbalance, due to strong adsorption of the products on the photocatalyst surface. No reactivity was observed in the presence of PW_{12} alone while PW_{11} induced only isomerization of the glucose.

1. Introduction

The search of alternative resources for synthesis of chemicals currently produced from non-renewable sources has directed the activities of researchers towards the use of different raw materials such as biomass [1]. It seems particularly interesting the use of lignocellulose (cellulose, hemi-cellulose and lignin) which can derive from agricultural wastes. Glucose, obtained from cellulose, can be used for the sustainable production of high value chemicals. To this aim, catalytic processes at high pressure and temperature, pyrolysis, gasification or conversion under supercritical conditions have been the object of scientific research. Glucose can be used to obtain ethanol by fermentation [2], sorbitol and mannitol by hydrogenation [3], 5-hydroxymethyl furfural by dehydrocyclization [4] and also to produce hydrogen [5]. Glucose is the monosaccharide most extensively studied in oxidation reactions particularly to obtain gluconic and glucaric acids [6]. This last reaction and in general, the selective oxidation of alcohols to their corresponding carbonyl compounds has attracted attention in the field of catalysis, due to its strategic importance [7]. Gluconic acid, with an annual estimated market of $6{\cdot}10^4$ ton, is used as a biodegradable chelating agent, a water soluble cleansing agent and an intermediate in food and pharmaceutical industries [8]. It is currently industrially prepared by fermentation of glucose by Aspergillus niger [9], although this process presents some drawbacks, as the disposal of dead microbes and the slow reaction rate. The heterogeneous catalytic oxidation of glucose has been presented as an attempt to overcome the problems of the biological process. The heterogeneous catalytic oxidations of sugars are performed by using supported noble metal catalyst in aqueous medium with batch reactors in the presence of air or oxygen under atmospheric pressure at temperatures of 293-353 K. The reaction is carried out at almost neutral or basic pH's (7-9) in order to allow the carboxylate anions to desorb from the catalyst surface avoiding their degradation [10]. The mild reaction conditions, along with the fact that the reactants are renewable and the products are environmentally benign because of their biodegradability, make the catalytic oxidation of carbohydrates a paradigm of green chemistry. Metal catalysts as Pt, Pd, Rh, Bi or Pb supported on TiO_2, Al_2O_3 or activated carbon have been used as catalysts but Au seems to be the most promising one [11-15]. Gold nanoparticles supported on activated carbon [16] or ZrO_2 [17] showed good catalytic activity for oxidation of glucose to gluconic acid at 50 °C in the presence of O_2 at pH's ranging between 8 and 10.

In this context, heterogeneous photocatalysis can be also considered as an alternative. The heterogeneous photocatalytic technology by using semiconductor oxides as photomediators is known as a process suitable to degrade organic and inorganic pollutants both in vapour and in liquid phases under very mild experimental conditions [18]. It is generally accepted that TiO_2 is the most reliable photocatalyst [19] and Colmenares et al. investigated the glucose photocatalytic oxidation in the presence of TiO_2 in acetonitrile-water suspensions [20-22]. They obtained

[a]*Schiavello-Grillone" Photocatalysis Group, Dipartimento di Energia, Ingegneria dell'informazione, e modelli Matematici (DEIM), Università degli Studi di Palermo, Viale delle Scienze Ed. 6, 90128, Palermo, Italy.*
[b]*Dipartimento Ingegneria Civile, Ambientale, Aerospaziale, dei Materiali, Viale delle Scienze, 90128 Palermo, Italy.*

Paper presented at FineCat 2015, Palermo, Italy, April 8-9, 2015.

Electronic Supplementary Information (ESI) available: [details of any supplementary information available should be included here]. See DOI: 10.1039/x0xx00000x

glucaric and gluconic acids along with arabitol and reported that the presence of acetonitrile stabilized the carboxylic acids by solvation suppressing their further oxidation [22]. It is rare to obtain acceptable selectivity values for partial photocatalytic oxidation reactions in the presence of only water as the solvent [23]. Chong et al. studied the conversion of glucose under anaerobic conditions in TiO_2-rutile aqueous suspensions and they found arabinose, erythrose and hydrogen as the products [24]. Heteropolyacid (HPA) clusters have been studied as homogeneous photocatalysts, due to their ability to absorb UV light. The absorption of light by the ground electronic state of the HPA produces a charge transfer-excited state HPA* which can behave as a better oxidant species than the corresponding ground states [25]. Under irradiation with light of suitable wavelengths HPA reduces to HPA^-, the so called "heteropoly-blue". The heteropoly-blue species is relatively stable, absorbs visible light and is readily reoxidized to the original HPA. This process can occur both with the plenary HPA Keggin species ($H_3PW_{12}O_{40}$) and with the lacunary Keggin cluster ($K_7PW_{11}O_{39}$) [26]. HPA photo-reduction has been proved to be synergistically enhanced in HPA/TiO_2 composites where photo-generated electrons can be transferred from the conduction band of TiO_2 to HPA. In this way the charge-pair recombination in the TiO_2 is delayed [27,28]. Heteropolyacids, such as $H_3PW_{12}O_{40}$, are also strong acid catalysts able to catalyze at low temperatures a wide range of catalytic processes [29]. They exhibit very strong Brönsted type acidity, making them suitable for various acidic reactions, such as esterification, transesterification, hydrolysis, Friedel-Crafts alkylation and acylation and Beckmann rearrangement [30].

The present paper reports the preparation of nanometer-sized TiO_2 particles by a solvothermal method. The commercial saturated $H_3PW_{12}O_{40}$ (labelled as PW_{12}) and the home prepared lacunary monovacant $K_7PW_{11}O_{39}$ Keggin salt (labelled as PW_{11}) were coupled by a solvothermal treatment with TiO_2 obtaining PW_{12}/TiO_2 and PW_{11}/TiO_2 composite materials. Moreover, also the impregnation of the saturated Keggin unit PW_{12} on commercial TiO_2 surface was performed for the sake of comparison. Some physico-chemical properties of the prepared materials were investigated along with their photoactivity for glucose oxidation in aqueous medium at natural pH. The experiments were carried out under mild conditions: room temperature, atmospheric pressure in aqueous suspensions and by using an inexpensive material. Photocatalysis by using heterogeneized heteropolyacids is a novel field, and the glucose partial oxidation by using these solids has never been investigated before, to the best of our knowledge.

2. Experimental

2.1 Photocatalysts preparation and characterization

A first set of powders was obtained by wet impregnation of commercial TiO_2 (Evonik P25) with a solution of a commercial heteropolyacid (HPA), i.e. tungstophosphoric acid $H_3PW_{12}O_{40}$ (Aldrich reagent grade 99.7%), labelled as PW_{12}. In particular TiO_2 (8.3 g) was added to a water solution (50 mL) containing the appropriate amount of PW_{12} (2.3 g). The suspension was stirred for ca. 1 h and then it was divided in two parts. One of them was hydrothermally treated in a teflonated autoclave for 48 hours at 200°C and the obtained white powder filtered and dried at 60°C. This sample has been named PW_{12}/P25 solv. The other part of the suspension was, instead, evaporated until dryness in a vacuum-dryer apparatus and the obtained powder labelled as PW_{12}/P25.

An alternative method was followed to obtain TiO_2 by using titanium isopropoxide, $Ti(OPr)_4$, (Aldrich 97%) as the precursor. The composite materials were prepared by adding the alkoxide precursor (32 mL) to the PW_{12} (2.3 g) aqueous solution (50 mL) and the resulting suspension was subjected to a hydrothermal treatment at 200°C for 48 h (in this case the system reached a pressure of ca. 17 atm). The resulting bluish powder was washed three times with hot water and finally filtered and dried at 60°C. This sample was denoted as PW_{12}/TiO_2 solv. The analogous bare TiO_2 was prepared under the same experimental conditions in the absence of PW_{12} and labeled as TiO_2 solv.

Another set of samples was prepared by using a monolacunary PW_{11} Keggin salt. The heteropolyacid $K_7PW_{11}O_{39}$ has been obtained by following the Haraguchi method [31]. 20 g of commercial $H_3PW_{12}O_{40}\cdot 26\ H_2O$ were dissolved in 100 mL of hot water, then 1.0 g of KCl was added and the pH of the solution adjusted to 5 with $KHCO_3$ 1 M. The obtained solid was filtered and dried at room temperature. For the preparation of the $K_7PW_{11}O_{39}/TiO_2$ materials, 3.6 mL of titanium isopropoxide was dissolved in 24 mL of 2-propanol under stirring at room temperature for 1 h. 0.125 or 0.250 g of $K_7PW_{11}O_{39}$ were dissolved in 2 mL of hot water and then added, under vigorous stirring, to the alcoholic solution of the TiO_2 precursor. The resulting suspension was adjusted to pH 5 with acetic acid 1 M, transferred to the teflonated autoclave and heated at 433 K for 48 h. The white bluish powder obtained was washed with water and eventually dried at room temperature. The obtained powders were named PW_{11}-X/TiO_2 solv (where X = 0.125 or 0.250 g, depending on the amount of PW_{11} used).

Bulk and surface characterizations were carried out in order to define some physicochemical properties of the powders. Their crystalline phase structure was determined at room temperature by powder X-ray diffraction analysis (PXRD) carried out by using a Panalytical Empyrean, equipped with CuKa radiation and PixCel1D (tm) detector. The specific surface areas (SSA) were determined in a Flow Sorb 2300 apparatus (Micromeritics) by using the single-point BET method. Scanning electron microscopy (SEM) was performed using a FEI Quanta 200 ESEM microscope, operating at 20 kV on specimens upon which a thin layer of gold had been evaporated. An electron microprobe used in an energy dispersive mode (EDAX) was employed to obtain information on the actual metals content present in the samples. Raman spectra were obtained by means of a BWTek-i-micro Raman Plus System, equipped with a 785 nm diode laser. The measurements were performed focusing the sample by a 20x magnification lens, spot size was around 50 µm. The accuracy of Raman shift was around 3 cm^{-1}. The power of the laser used was 15% of the maximum value that was around 300 mW. Infrared spectra of the samples in KBr (Aldrich) pellets were obtained with a FTIR-8400 Shimadzu spectrophotometer and the spectra were recorded with 4 cm^{-1} resolution and 256 scans. The diffuse reflectance spectra (DRS) were recorded in air at room temperature in the 250-800 nm wavelength range using a Shimadzu UV-2401 PC spectrophotometer, with $BaSO_4$ as the reference material.

2.2 Photocatalytic activity

The photoreactivity runs were carried out at room temperature and ambient pressure in a 800 mL open reactor irradiated in the UV region with an immersed 125 W medium pressure Hg lamp (Helios Italquartz, Italy). The initial aqueous glucose concentration was 1 mM and the runs were carried out at natural pH. The impinging radiation intensity was measured by a radiometer Delta Ohm

DO9721, and it was 5.5 mW/cm^2. The amounts of photocatalyst needed to absorb all the photons emitted by the lamp in the reacting suspension was checked by using the same radiometer and depended on the catalyst used. In particular, in some cases 0.3 g/L of catalyst were sufficient (see TiO_2 P25, PW_{12}/P25 solv and PW_{12}/P25), whereas in other cases the amount was 2.0 g/L (see TiO_2 solv, PW_{11}-0.125/TiO_2 solv and PW_{11}-0.250/TiO_2 solv) or 2.8 g/L (see PW_{12}/TiO_2 solv).

Air was not bubbled during the experiments but the vessel was just opened in ambient conditions. The values of substrate concentration before the addition of catalyst and before the starting of irradiation were measured in order to determine the substrate adsorption on the catalyst surface under dark conditions. During the photoreactivity runs samples were withdrawn at fixed times and immediately filtered through 0.2 µm membranes (HA, Millipore) before analyses. The quantitative determination and identification of glucose and its degradation products were performed by means of a Thermo Scientific Dionex ultimate 3000 HPLC equipped with a Diode Array and refractive index detectors. The column was a REZEK ROA Organic acid H^+ Phenomenex, the eluent an aqueous 2.5 mM H_2SO_4 solution and the flow rate 0.6 mL min^{-1}. Retention times and UV spectra of the compounds were compared with those of standards purchased from Sigma-Aldrich with a purity of >99%. All of the runs lasted ca. 6 h and were performed at least twice.

In order to test the adsorption extent of some reaction intermediates (arabinose and gluconic acid) on the different photocatalysts used, some adsorption tests were carried out following the procedure below reported. An amount of 2.8 g·L^{-1} of photocatalyst was dispersed in an aqueous solution containing 1 mmol·L^{-1} of arabinose or 1 mmol·L^{-1} of gluconic acid. The suspension was maintained under stirring in dark condition for 6 h. 5 ml of suspension were withdrawn every hour and the concentrations of arabinose or gluconic acid were analysed after the separation of the photocatalyst.

3. Results and Discussion

3.1 Characterization of the photocatalysts

Table 1 reports some physicochemical features of the powders investigated as photocatalysts. The specific surface area (SSA) of TiO_2 sample prepared under solvothermal conditions was 260 m^2·g^{-1}, a value much higher than that of the commercial TiO_2 Evonik P25 (50 m^2·g^{-1}). The SSA's of the commercial PW_{12} and the home prepared PW_{11} were 15 and 80 m^2·g^{-1}, respectively, and as a general trend, those of all of the composite materials were smaller than those of the bare TiO_2 samples.

XRD diffractograms of all of the prepared samples are reported in Figure 1. In Figure 1 (A) the diffractograms correspond to the bare PW_{12}, commercial TiO_2 Evonik P25 (in the following named only TiO_2 P25) and the composites obtained with these two substances. The PW_{12} presents a crystalline structure and the commercial TiO_2 P25 consists of anatase and rutile polymorphs. In the composite materials, new peaks, attributable to the heteropolyacid, in addition to those of TiO_2 are present and they are less intense in the PW_{12}/P25 solv sample than in the PW_{12}/P25 one. This finding can account for the best dispersion of HPA in the material prepared solvothermically. Indeed, the more defined peaks can be due to the heterogeneity of the dispersion of PW_{12} in the P25 impregnated sample, as confirmed by SEM (see in the following). Figure 1 (B) shows the diffractograms of PW_{12} along with the home prepared bare TiO_2 and the composite PW_{12}/TiO_2 solv prepared solvothermically. In the diffractogram it can be noticed the presence of anatase phase for both bare TiO_2 and PW_{12}/TiO_2 solv samples without significant differences and without the presence of peaks ascribable to HPA. This result suggests a good statistic mixing of HPA with TiO_2. Figure 1 (C) reports the diffractograms of PW_{11}, TiO_2 solv and PW_{11}-X/TiO_2 solv samples (see Experimental section for the meaning of the code). The diffractogram of bare PW_{11} indicates a good crystallinity of this sample although the characteristic peaks have not been reported in the literature. Both PW_{11}-X/TiO_2 solv samples do not present a strong evidence of the PW_{11} crystalline phase segregated. The only significant difference between PW_{11}-0.125/TiO_2 solv and PW_{11}-0.250/TiO_2 solv samples and TiO_2 solv is the wide peak localized at 2θ= 14°.

The samples were also investigated by FTIR (spectra not reported for the sake of brevity) to check the structural integrity of the Keggin unit after the preparation of the HPA/TiO_2 composites. The arrangement structure of the PW_{12} consists of a PO_4 tetrahedron surrounded by four W_3O_9 groups formed by edge sharing octhaedra [32]. This arrangement gives rise to four stretching bands: P-O stretching mode at 1080 cm^{-1}, W=O stretching observed at 990 cm^{-1} and two peaks at ca. 910 cm^{-1} and 810 cm^{-1} attributed to two types of W-O-W units [33]. It is difficult to characterize the Keggin structure in the composites by IR spectroscopy because some of the bands overlap with those assigned to TiO_2 powder; the latter, in fact, presents an intense and broad vibration band originated from Ti–O–Ti bonds located at wavenumbers lower than 900 cm^{-1}.

Table 1. Some physicochemical data concerning the characterization of the TiO_2 and HPA/TiO_2 photocatalysts

			Nominal		EDAX	
Photocatalyst	S.S.A. [m^2/g]	E_{gap} [eV]	W atomic [%]	Ti atomic [%]	W atomic [%]	Ti atomic [%]
TiO_2 P25	50	3.2	-	-	-	-
PW_{12}	15	3.2	-	-	-	-
PW_{12}/P25	48	3.0	9	91	10±1*	90±1*
PW_{12}/P25 solv	43	3.0	7	93	7±1	93±1
TiO_2 solv	260	3.2	-	-	-	-
PW_{12}/TiO_2 solv	176	3.2	7	93	10±0.1	90±0.1
PW_{11}	80	3.4	-	-	-	-
PW_{11}-0.125/TiO_2 solv	206	3.1	4	96	5±1	95±1
PW_{11}-0.250/TiO_2 solv	196	3.2	7	93	7±1	93±1

*Some agglomerates in the PW_{12}/P25 sample present values of W atomic percentage and Ti atomic percentage of ca. 30% and ca. 70%, respectively.

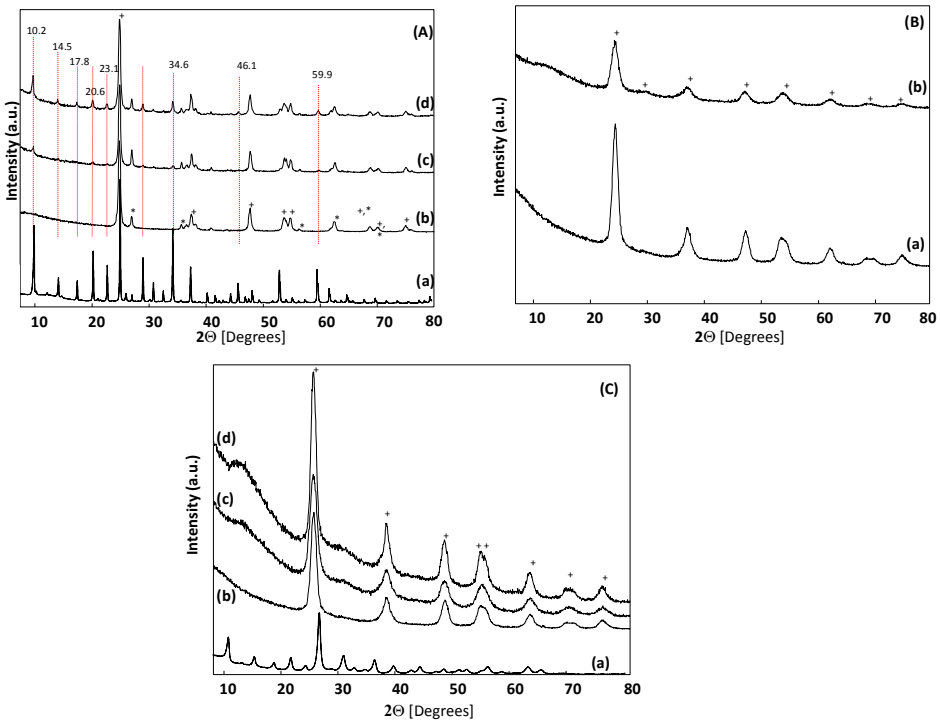

FIGURE 1. XRD patterns of the photocatalysts: (A) (a) PW_{12}; (b) TiO_2 P25; (c) PW_{12}/P25 solv; (d) PW_{12}/P25; (B) (a) TiO_2 solv; (b) PW_{12}/TiO_2 solv and (C) (a) PW_{11}; (b) TiO_2 solv; (c) PW_{11}-0.125/TiO_2 solv; (d) PW_{11}-0.250/TiO_2 solv. (⁎ Rutile; + Anatase).

Raman spectroscopy allowed a much better understanding of the structural modifications induced at the surface. In Figure 2(A) both bare TiO_2 samples (TiO_2 solv and TiO_2 P25) show Raman peaks centered at 144, 197, 399, 513, and 639 cm^{-1} attributable to the E_g, E_g, B_{1g}, A_{1g} and B_{2g} modes of anatase TiO_2 [34]. On the contrary, the characteristic peaks of the rutile phase, that should be located at 444 and at 609 cm^{-1}, are not observed in the samples, as reported before [27], probably because the rutile crystallites observed by XRD are located in the bulk of the material.

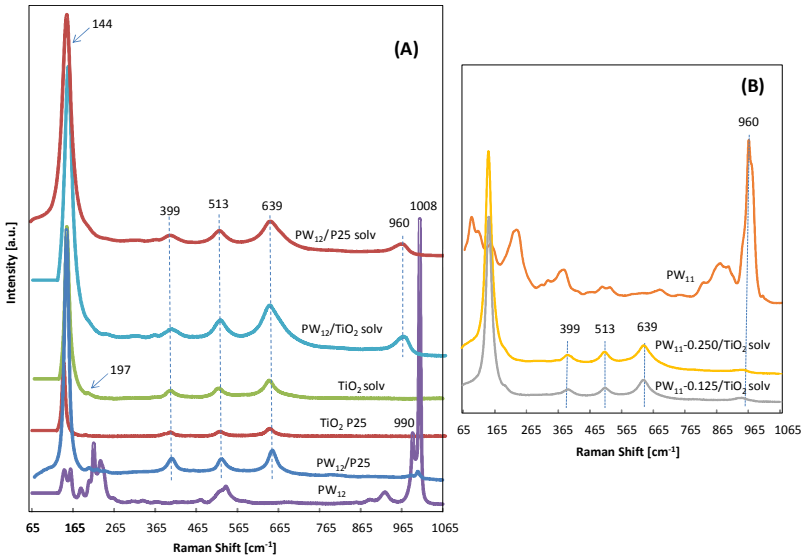

FIGURE 2. Raman spectra of the samples: (A) bare TiO_2 and PW_{12} containing materials, and (B) PW_{11} containing samples.

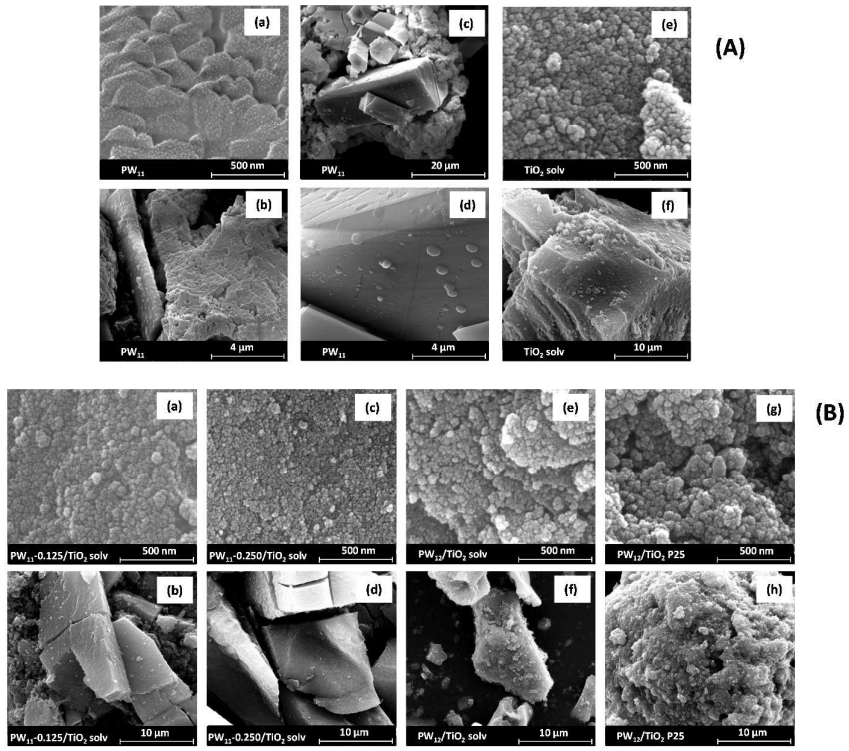

FIGURE 3. SEM microphotographs of (A) two agglomerates (a, b and c, d) of bare PW_{11} and (e, f) bare TiO_2 at different magnifications and (B) (a-h) some selected composite materials at two different magnifications: (a, b) PW_{11}-0.125/TiO_2 solv; (c, d) PW_{11}-0.250/TiO_2 solv; (e, f) PW_{12}/TiO_2 solv; (g, h) PW_{12}/TiO_2 P25.

The Raman spectrum of PW_{12} shows a sharp and intense band at 1008 cm^{-1} and a peak at 990 cm^{-1} assigned to P–O vibrations and bands at lower wavenumbers, attributed to W–O (925 cm^{-1}) and W–O–W (880 cm^{-1}) vibrations [33].

In the HPA/TiO_2 composites the Raman peaks attributable to anatase phase are also present indicating that the crystalline form is preserved on the surface after the introduction of the heteropolyacid. The four HPA characteristic bands are not present due to the very low amount of HPA in the samples. However, the sharper and more intense band at 1008 cm^{-1} and the shoulder at 990 cm^{-1} are present for the PW_{12}/P25 composite in Figure 2(A) and no significant shift can be observed. On the contrary, for the samples treated by the solvothermal method, PW_{12}/P25 solv and PW_{12}/TiO_2 solv, the 1008 and 990 cm^{-1} peaks appear as a unique broad peak shifted to ca. 960 cm^{-1}. These finding can be attributed to an interaction between the oxygen atom of the Keggin anion and the hydroxyl groups on the TiO_2 surface [35]. As far as the lacunary Keggin is concerned, Figure 2(B) shows the high complexity of the Raman spectrum of this HPA. The spectra of the binary PW_{11}/TiO_2 samples confirm the presence of anatase along with a small shoulder at ca. 940 cm^{-1} due to the presence of PW_{11} in the composites (see the intense band observed for the bare PW_{11} at 960 cm^{-1}).

SEM microphotographs of some selected materials are reported in Figures 3(A) and (B). In particular, Figure 3(A) reports some pictures of the bare PW_{11} (a-d) and of the home prepared TiO_2 (e-f) samples whereas Figure 3(B) reports some pictures of composite powders. The morphology of the PW_{11} salt appears completely different compared with that of the other samples. This sample seems consisting of very large crystals surrounded by others growing small crystals. On the contrary, the TiO_2 sample which was solvothermally prepared consists of agglomerates of primary particles (ca. 40-60 nm), whose size ranges between 2.5 and 30 µm. The PW_{11}-0.125/TiO_2 solv, PW_{11}-0.250/TiO_2 solv and PW_{12}/TiO_2 solv composite samples (Figure 3(B) a-b, c-d and e-f, respectively) appear very similar to the bare TiO_2 sample (Figure 3(A) e-f), indicating that the small content of PW_{11} or PW_{12} did not modify the morphology of the majority component TiO_2. From the perusal of Figures 3(A) and (B) it can be concluded that in the case of the PW_{11}-0.250/TiO_2 solv the size of the primary particles resulted smaller (ca. 20 nm). Consequently, it seems that the presence of a higher amount of PW_{11} caused a decrease of the size of the primary particles. The morphology of PW_{12}/P25 (Figure 3(B) g-h) and PW_{12}/P25 solv (not reported in Figure 3), is very similar to the bare material (SEM picture of bare TiO_2 P25 has been already reported [28]). The agglomerates of these particles present the same shape and consist

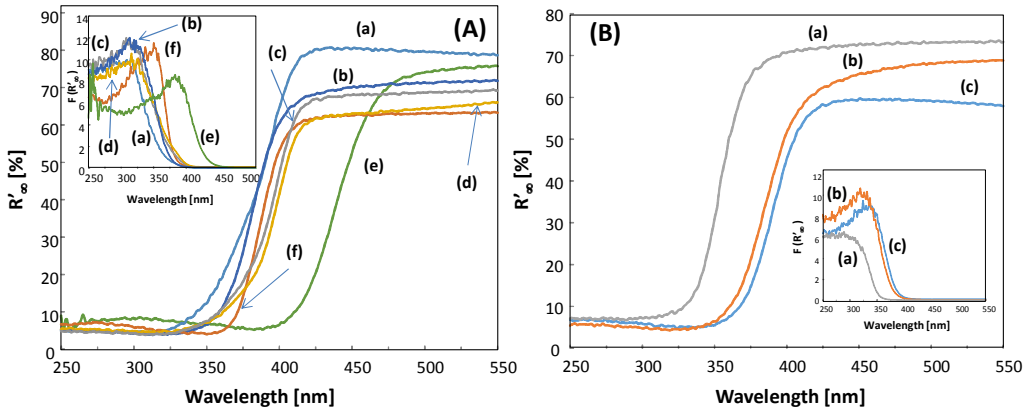

FIGURE 4. Diffuse reflectance spectra of the samples: (A) (a) TiO_2 P25; (b) TiO_2 solv; (c) PW_{12}/P25; (d) PW_{12}/P25 solv; (e) PW_{12}/TiO_2 solv; (f) PW_{12} and (B) (a) PW_{11}; (b) PW_{11}-0.125/TiO_2 solv, and (c) PW_{11}-0.250/TiO_2 solv. The insets report the absorbance spectra obtained by applying the Kubelka-Munk function, $F(R_\infty)$, to the diffuse reflectance spectra.

of nanoparticles with similar sizes (ca. 50 nm). Table 1 reports the nominal and the average EDAX values of atomic percentage of W in PW_{11} or PW_{12} and the atomic percentage of Ti in the TiO_2. EDAX measurements confirmed a homogeneous content of the HPAs onto the catalyst with the exception of the PW_{12}/P25 sample where tungsten was present in some agglomerates in much higher content with respect to the nominal one. In all of the other samples, the measured amount of W and Ti was always very close to the nominal one. Figure 4 (A) and (B) report the diffuse reflectance UV-Vis spectra (DRS) of the bare TiO_2 and HPA/TiO_2 composite samples. The insets report the absorbance spectra obtained by applying the Kubelka-Munk function, $F(R_\infty)$, to the diffuse reflectance spectra. All of the spectra are characterized by a charge transfer process, from O 2p to Ti 3d for TiO_2 or to HOMO-LUMO transition for the HPAs.

Figure 4 (A) reports the spectra of the bare TiO_2 and PW_{12}/TiO_2 solv samples, whereas in Figure 4 (B) those concerning the samples prepared with the lacunary HPA are shown. The spectrum of PW_{11} evidences a higher energy for the transition HOMO-LUMO compared to that of PW_{12}. The Kubelka-Munk function $F(R_\infty)$ has been used to obtain the Tauc plots [36] where the extrapolation in the linear fitting of the plot $(F(R_\infty)\cdot E)^{1/2}$ vs incident light energy in eV gives the band gap energy (see Table 1). The presence of the HPA gave rise to a slight increase of the band gap energy, particularly where the PW_{11} was present. Based on the above physico-chemical characterization results, it can be concluded that the primary Keggin structure of the saturated and lacunary HPA remained virtually unchanged after the deposition of the cluster on the oxide surface. Different kind of interactions between the saturated or lacunary Keggin unit and the TiO_2 surface can be hypothesized. For the PW_{12}/TiO_2 solv composite, it can be suggested that the saturated Keggin unit interacts with TiO_2 by hydrogen bonding and acid-base reaction as reported before [35]. On the contrary, according to Ma et al., the removal of a tungsten–oxygen octahedral from a saturated $PW_{12}O_{40}^{3-}$ gives rise to the lacunary anion ($PW_{11}O_{39}^{7-}$) that results highly nucleophilic and can reacts easily with electrophilic groups such as titanium atoms of Ti-OH groups present in TiO_2. Therefore, in the PW_{11}/TiO_2 composite, $K_7PW_{11}O_{39}$ presents vacant sites, which allow connecting two TiO_4 units of the TiO_2 network to make up tungsten-oxygen octahedral lacunas. Consequently, the terminal nucleophilic oxygen atoms of the $K_7PW_{11}O_{39}$ become bridge atoms that allow to connect PW_{11} and TiO_2 via W-O-Ti bonds [37].

3.2 Glucose photocatalytic conversion

Figures 5-7 report the results of the photocatalytic glucose conversion in the presence of different catalysts. Figure 5 reports the activity of the bare TiO_2 powders. By using TiO_2 P25, the decrease of glucose concentration was accompanied by the appearance of various compounds, mainly formic acid and arabinose. Other oxidation products as erythrose and gluconic acid were also formed in lower amounts. Fructose, a glucose isomerization product, has been also found. It is worth to mention that the amount of P25 sufficient to absorb all the photons emitted by the lamp was 0.3 g/L, under the experimental conditions used. TiO_2 solv possesses a lower ability in absorbing photons (this feature can be related to the higher granulometry of the powder) and 2 g/L were necessary to absorb all the emitted photons. Consequently, two runs with TiO_2 solv were carried out: the first one with 2 g/L, the second one with 0.3 g/L. As reported in Figure 5, for the run with 2 g/L of photocatalyst, the decrease of glucose concentration was faster than in the presence of TiO_2 P25, but the amount of formic acid was much lower. Arabinose was found as a product, along with low amounts of erythrose and gluconic acid. In this case, the isomerization product fructose was also observed. By employing a lower amount of TiO_2 powder (0.3 g/L) the glucose conversion decreased, the quantities of formic acid, erythrose and gluconic acid slightly decreased and arabinose was completely absent. Only the fructose concentration increased moderately.

Table 2 reports conversion and selectivity to the different species found along with the carbon mass balance calculated after 6 hours of irradiation for the experiments reported in Figure 5. The glucose conversion, X, and the selectivity, S, to fructose, gluconic acid, arabinose and erythrose have been calculated as follows:

$$X = ([glucose]_i - [glucose]) / [glucose]_i \times 100 \quad (1)$$

$$S = [product]/ ([glucose]_i - [glucose]) \times 100 \quad (2)$$

Journal Name

ARTICLE

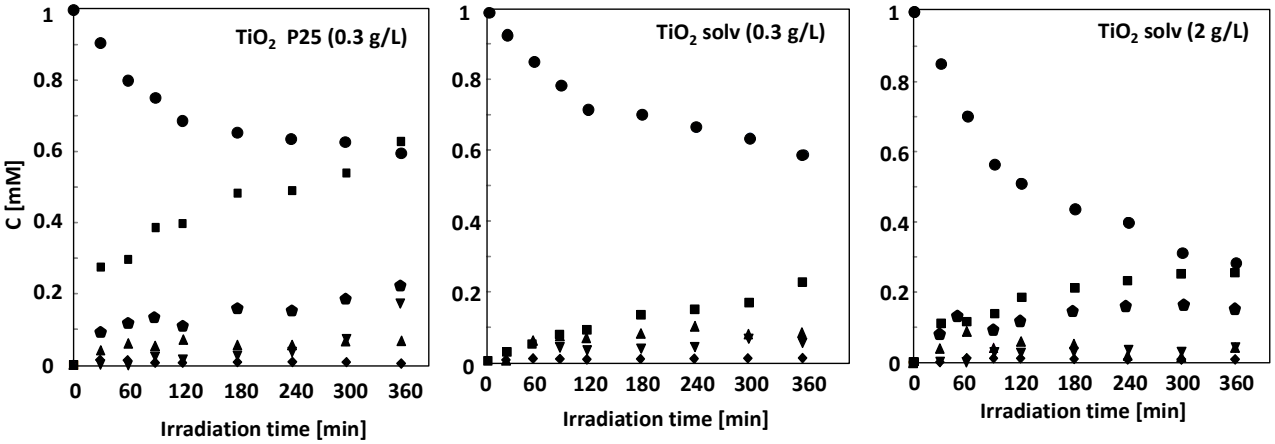

FIGURE 5. Evolution of glucose and photocatalytic reaction products versus irradiation time in the presence of bare TiO_2 samples. (●) glucose, (▲) fructose, (▼) erythrose, (⬟) arabinose, (◆) gluconic acid, and (■) formic acid. The average oscillation percentage of the experimental data was ca. ± 2%.

where $[glucose]_i$ is the initial glucose concentration, [glucose] the concentration after 6 hours of irradiation and [product] denotes the product concentration analysed at the same time. It is important to highlight that the carbon atom mass balance has been satisfied when bare TiO_2 P25 has been used but not in the presence of the bare home prepared TiO_2 solv sample. In fact, the color of the latter sample turned pale orange after all of the runs, indicating that some species remained strongly adsorbed on its surface. The greater ability of TiO_2 solv sample to adsorb the reaction intermediates compared to that of TiO_2 P25 sample has been confirmed by adsorption tests carried out in the presence of arabinose and in the presence of gluconic acid chosen as representative intermediates. These tests indicate that the TiO_2 solv sample was able to adsorb the compounds above mentioned ca. seven times more than TiO_2 P25 sample.

Figure 6 reports the evolution of glucose and reaction products in photocatalytic experiments carried out in the presence of PW_{12}/TiO_2 composites. The samples obtained by impregnation of TiO_2 P25 with PW_{12}, i.e. PW_{12}/P25 and PW_{12}/P25 solv, convert glucose faster than the correspondent bare TiO_2 P25. In both cases fructose was the main species observed during the run, but also a significant amount of gluconic acid was formed, particularly in the presence of PW_{12}/P25 solv. It is worth noting that the amount of gluconic acid formed by using these two composite materials was always higher than that observed in the presence of bare TiO_2 P25. Small amounts of formic acid and erythrose were also found along with traces of glucaric acid. By using PW_{12}/TiO_2 solv as the photocatalyst (2.8 g/L were needed to absorb all the photons emitted by the lamp), the conversion of glucose was lower with respect to PW_{12}/P25 and PW_{12}/P25 solv. Fructose resulted to be the main species, along with gluconic acid and formic acid. Table 3 collets the X, S and B data obtained for the runs reported in Figure 6. The presence of PW_{12} along with TiO_2 P25, in both samples obtained by impregnation or by solvothermal treatment, caused an increase in the glucose conversion, the absence of arabinose and a strong decrease of formic acid and erythrose in comparison to TiO_2 P25 (see Table 2).

TABLE 2. Photoreactivity assessment of bare TiO_2 powders: glucose conversion, X, selectivity to the identified reaction products, S, and carbon mass balance, B, after 360 minutes of irradiation.

		TiO_2 P25 (0.3 g/L)	TiO_2 solv (0.3 g/L)	TiO_2 solv (2 g/L)
X [%]	Glucose	41±1	40±1	72±1
S [%]	Fructose	14±1	20±1	6±0.5
	Gluconic acid	0.6±0.1	3±0.2	1±0.1
	Arabinose	42±2	-	26±1
	Erythrose	28±1.5	13±1	5±0.5
B [%]	Carbon	99±1	75±2	55±1

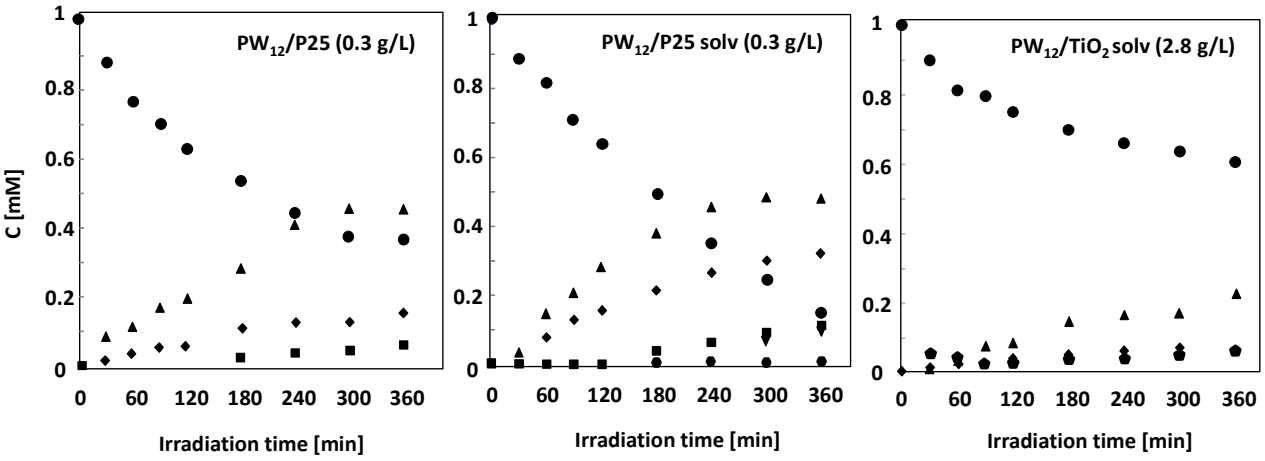

FIGURE 6. Evolution of glucose and their photocatalytic reaction products versus irradiation time in the presence of the binary materials composed of PW_{12} and TiO_2. (●) glucose, (▲) fructose, (▼) erythrose, (⬟) arabinose, (◆) gluconic acid, (⬣) glucaric acid, and (■) formic acid. The average oscillation percentage of the experimental data was ca. ± 2%.

On the contrary, conversion to fructose and gluconic acid increased. In particular, in the presence of PW_{12}/P25 solv the amount of valuable gluconic acid was the highest obtained in this work. Notably this last sample did not give rise to leaching of PW_{12} in the liquid phase, contrary to what observed for PW_{12}/P25 prepared by impregnation.

In the light of the results above presented, some general considerations can be done. The presence of PW_{12} in PW_{12}/P25 and PW_{12}/P25 solv samples, resulted beneficial. On the contrary, PW_{12}/TiO_2 solv composite showed a lower reactivity than that obtained in the presence of PW_{12}/P25 samples giving rise mainly to fructose. This finding can be explained by taking into account the different preparation methods used to obtain this composite in comparison to those containing P25.

In the latter cases, PW_{12} was added to TiO_2 already crystallized, whereas PW_{12}/TiO_2 solv sample was prepared by adding the Ti organometallic precursor to the PW_{12} solution; consequently, PW_{12} was dispersed not only on the TiO_2 surface but mainly in the bulk. This fact has been evidenced by XRD investigations where the pattern of the PW_{12}/TiO_2 solv does not indicate the presence of the heteropolyacid. Consequently, it is evident that the presence of PW_{12} on the TiO_2 P25 surface, both prepared by impregnation or solvothermically, was able to modify the reactivity and selectivity of the bare TiO_2 towards the formation of less degraded products in the glucose oxidation process. Also in the PW_{12}/TiO_2 solv sample the presence of PW_{12} in the bulk of TiO_2 influenced the reactivity of TiO_2 giving rise to a decrease in the formation of formic acid and an increase of fructose.

Moreover, the presence of PW_{12} favoured the products desorption from the photocatalyst surface making possible the achievements of the carbon mass balance contrarily to what observed with the bare TiO_2 solv sample. Adsorption tests carried out as those discussed for TiO_2 P25 and TiO_2 solv sample indicated that the presence of PW_{12} drastically reduced the adsorption ability of TiO_2 solv. This finding was also observed in the presence of PW_{11}, as it will be discussed later. It is worth to mention that both HPA species, PW_{11} and PW_{12}, are soluble in water. PW_{12} used as photocatalyst in homogeneous regime did not show to be photoactive; conversely, PW_{11} gave rise to a slight conversion of glucose to fructose. The products formed in the presence of samples consisting of the PW_{11} lacunary cluster and TiO_2 (PW_{11}-0.125/TiO_2 solv and PW_{11}-0.250/TiO_2 solv) are reported in Figure 7. Also for these two samples different amounts were used (0.3 g/L and 2 g/L), due to their scarce ability to absorb all the photons emitted by the lamp.

Table 3. Photoreactivity assessment of composites containing PW_{12} and TiO_2: glucose conversion, X, selectivity to the identified reaction products, S, and carbon mass balance, B, after 360 minutes of irradiation.

		PW_{12}/P25 (0.3 g/L)	PW_{12}/P25 solv (0.3 g/L)	PW_{12}/TiO_2 solv (2.8 g/L)
X [%]	Glucose	64±1	85±1	39±1
S [%]	Fructose	68±2	55±2	56±2
	Gluconic acid	22±1	34±1	20±1
	Glucaric acid	-	1.5±0.2	-
	Erythrose	-	11±1	-
B [%]	Carbon	97±1	99±1	92±1

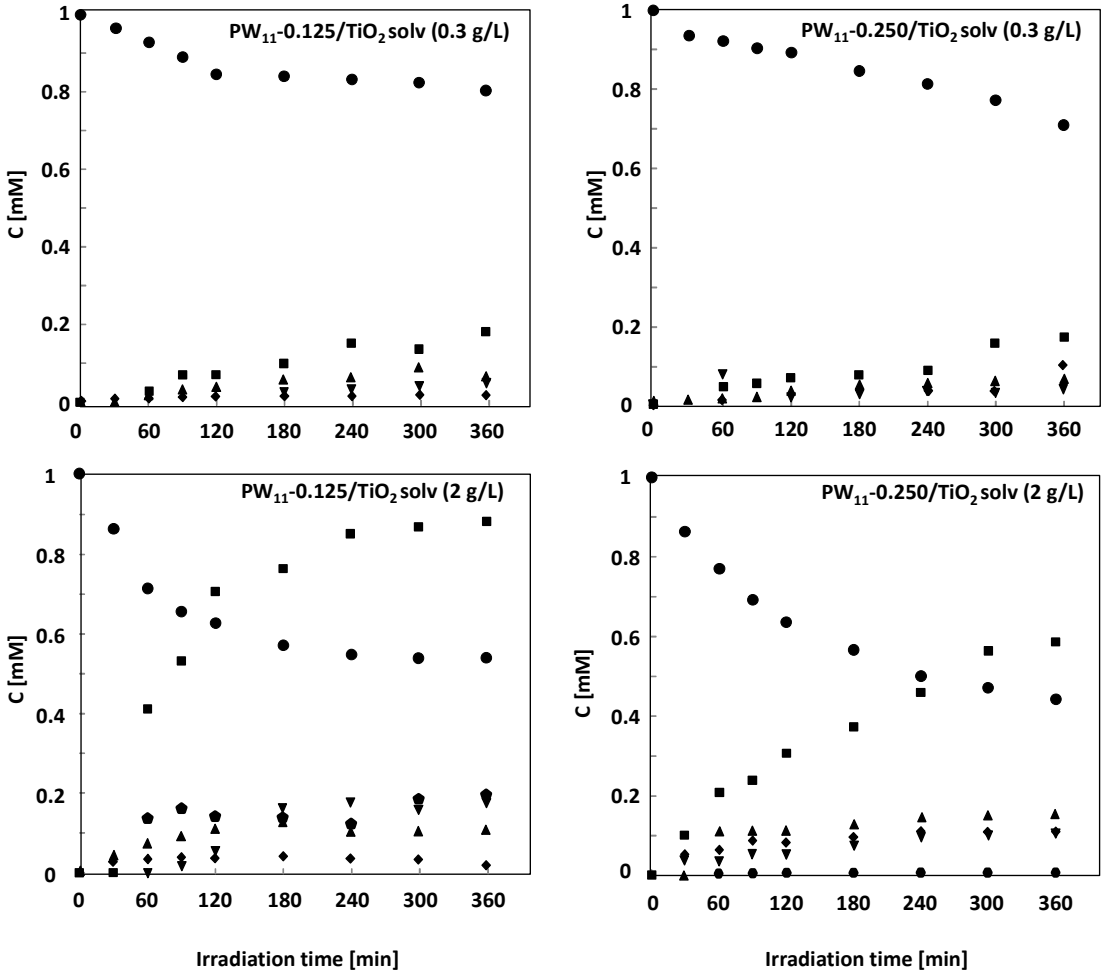

FIGURE 7. Evolution of glucose and their photocatalytic reaction products versus irradiation time in the presence of the binary materials composed of PW_{11} and TiO_2. (●) glucose, (▲) fructose, (▼) erythrose, (⬟) arabinose, (◆) gluconic acid, (⬣) glucaric acid, and (■) formic acid. The average oscillation percentage of the experimental data was ca. ± 2%.

No leaching of PW_{11} occurred during the experiments, indicating that PW_{11} played a role exclusively in heterogeneous phase. In the runs carried out with 0.3 g/L, the materials were scarcely active (see Figure 7) and some decrease in the concentration of glucose was observed along with the formation of small amounts of fructose, gluconic acid, erythrose and formic acid. The use of 2 g/L of photocatalyst gave rise to a high increase of reactivity. PW_{11}-0.250/TiO_2 solv converted glucose faster than PW_{11}-0.125/TiO_2 solv but in both cases the most important product was formic acid that was surprisingly found in higher amount in the presence of the latter sample. In both systems, the presence of gluconic acid, erythrose and fructose was also detected. The reactivity of this two photocatalysts differed only because arabinose was found in the presence of PW_{11}-0.125/TiO_2 solv while small amounts of glucaric acid were detected in the PW_{11}-0.250/TiO_2 solv. For the composite PW_{11}/TiO_2 solv samples the conversion of glucose was lower than for TiO_2 solv, whereas the selectivity to gluconic acid higher. The largest amount of photocatalyst (2 g/L vs. 0.3 g/L) caused a higher conversion of glucose but also a higher formation of formic acid.

It is worth noting that the presence of PW_{11} in the composite PW_{11}/TiO_2 solv samples favoured the desorption of the products from the photocatalyst surface, however it caused a strong increase of the overoxidation product, i.e. gluconic acid and formic acid.

On the basis of the previous considerations we can conclude that the presence of HPA (PW_{12} or PW_{11}) changed the glucose reaction mechanism; indeed, in the runs carried out by using bare TiO_2 the main products were arabinose and erythrose, whereas fructose and gluconic acid were preferentially formed when the PW_{12} composites were used as photocatalysts. When the PW_{11} composites were employed, the formation of formic acid was favoured. Probably, HPA modified the surface properties of TiO_2 and in particular the type and the strength of acid site along with their distribution. This finding can justify the higher amounts of fructose obtained when composite catalysts containing PW_{12} were used. Indeed, in the literature it is reported that the isomerization of glucose to fructose is catalysed by Lewis acids [38]. In particular, this effect was evident in the case of P25/TiO_2 samples where HPA

Table 4. Photoreactivity assessment of composites containing PW_{11} and TiO_2: glucose conversion, X, selectivity to the identified products, S, and carbon mass balance, B, after 360 minutes of irradiation.

		PW_{11} (0.3 g/L)	PW_{11}-0.125/TiO_2 solv (2 g/L)	PW_{11}-0.250/TiO_2 solv (2 g/L)	PW_{11}-0.125/TiO_2 solv (0.3 g/L)	PW_{11}-0.250/TiO_2 solv (0.3 g/L)
X [%]	Glucose	20±1	44±2	53±2	20±1	28±1
S [%]	Fructose	99±1	24±1	31±1	34±1	24±1
	Gluconic acid	-	4±0.2	19±1	9±0.5	35±2
	Glucaric acid	-	-	1±0.1	-	-
	Arabinose	-	38±2	-	-	-
	Erythrose	-	37±1	19±1	23±1	16±1
B [%]	Carbon	99±1	99±1	90±1	95±1	95±1

is preferentially localized on the TiO_2 surface. The presence of PW_{12} was able to change the reaction mechanism, probably because it modified the acid properties of the catalyst surface. This finding indicate that PW_{12} was able to explicate its acid function (see the higher formation of fructose) reducing the oxidizing ability of TiO_2 (see the disappearance of arabinose and erythrose and the formation of gluconic acid). Indeed, when TiO_2 was used alone, according to Chong et al [24], the most favoured reactions were due to the α scission (C_1-C_2 cleavage) giving rise to the formation of arabinose, erythrose and glyceraldehyde (this last observed only in traces). On the other hand, the oxidation of glucose to gluconic acid (as first step) and to glucaric acid (as second step) were observed only during the runs carried out by using PW_{12} containing composite photocatalysts. On the contrary, the presence of PW_{11}, that does not show any acid function, induces an increase of the oxidizing ability of TiO_2, probably acting through the formation of the heteropoly-blue species [26] and consequently reducing the electron-hole recombination on TiO_2. However, it is worth noting that the sample PW_{11}-0.125/TiO_2 solv is more oxidizing than the sample PW_{11}-0.250/TiO_2 solv. This fact can be explained by considering that an increase of the amount of PW_{11} over a certain value could cover the TiO_2 surface or favour the electron-hole recombination (two effects that in any case are detrimental for the reactivity). It is worth to remark that an important feature in the catalytic oxidation of carbohydrate molecules is the regio- and chemoselectivity, but these aspects have been considered out of the scope of this work. In Scheme 1 it has been summarized a possible reaction sequence by considering the Hoffman structures of the analysed molecules in the D-form.

The oxidation of glucose can occur by the oxidation of the anomeric center (C1) giving rise to gluconic acid. Successively, an oxidative attack to the C2 carbon gives rise to a formation of formic acid and arabinose. A further oxidative attack to the C2 carbon in arabinose molecule releases another formic acid molecule and erythrose, and in turn, the erythrose molecule can be transformed into glyceraldehyde (analysed in traces) by an oxidative attack. Finally formic acid, as the over-oxidation species, was obtained. The presence of glucaric acid has been also observed indicating the oxidation of both C1 and C6 atoms of glucose. The contemporaneous or successive oxidation of C1 and C6 can be explained by considering different glucose adsorption modes on the surface of the photocatalysts. The primary oxidation at the C6 of glucose to give glucuronic acid, reported in literature as one of the intermediates in catalytic oxidation of glucose [1], was not observed under the experimental condition used in this work, however in scheme 1 it has been also hypothesized, and represented in brackets.

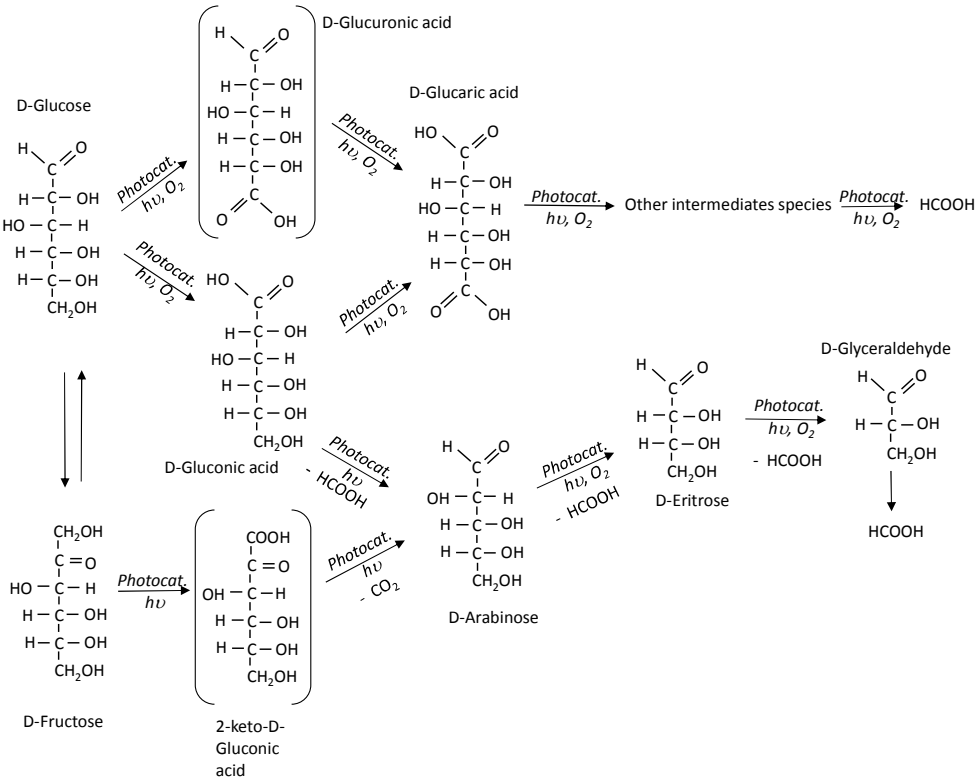

Scheme 1. Hypothesis of reaction sequence for the photocatalytic glucose oxidation.

Conclusions

We can conclude that, although fructose, gluconic acid, arabinose, erythrose and formic acid were observed as oxidation products when bare TiO_2 or HPA/TiO_2 composite materials were used, depending on the photocatalyst used a different reaction extent and distribution of intermediate oxidation products were observed. Moreover, traces of glucaric acid and glyceraldehyde were also found in some runs. The presence of PW_{12} or PW_{11} in the composite material influenced the reaction mechanism although no reactivity was observed in the presence of bare PW_{12}, whereas bare PW_{11} induced only isomerization of the glucose.

The C mass balance was virtually accomplished in the presence of commercial TiO_2 P25 and all of the HPA/TiO_2 composites. The experiments carried out in the presence of samples containing TiO_2 solvothermically prepared, instead, indicated a carbon unbalance, due to strong adsorption of reaction products on the photocatalyst surface.

References

1. A. Corma, S. Iborra, A. Velty, *Chem. Rev.*, 2007, **107**, 2411.
2. Y. Lin, S. Tanaka, *Appl. Microbiol. Biotechnol.*, 2006, **69**, 627.
3. R. Geyer, P. Kraak, A. Pachulski, R. Schödel, *Chem. Ing. Tech.*, 2012, **84**, 513.
4. J.N. Chheda, Y. Roman-Leshkov, J.A. Dumesic, *Green Chem.*, 2007, **9**, 342.
5. R.R. Davda, J.W. Shabaker, G.W. Huber, R.D. Cortright, J.A. Dumesic, *Appl. Catal. B*, 2005, **56**, 171.
6. M. Comotti, C.D. Pina, M. Rossi, *J. Mol. Catal. A*, 2006, **251**, 89.
7. T. Mallat, A. Baiker, *Chem. Rev.*, 2004, **104**, 3037.
8. S. Ramchandran, P. Fontanille, A. Pandey, C. Larroche, *Food Technol. Biotechnol.*, 2006, **44**, 185.
9. J.Z. Liu, L.P. Weng, Q.L. Zhang, H. Xu, L.N. Ji, *Biochem. Eng. J.*, 2003, **14**, 137.
10. M. Besson, P. Gallezot, *Catal. Today*, 2000, **57**, 127.
11. C. Baatz, B. Thielecke, Y. Prüße, *Appl. Catal. B*, 2007, **70**, 653.
12. S. Hermans, M. Devillers, *Appl. Catal. A*, 2002, **235**, 253.
13. N. Thielecke, K.D. Vorlop, U. Prüße, *Catal. Today*, 2007, **122**, 266.
14. M. Comotti, C. Della Pina, E. Falletta, M. Rossi, *J. Catal.*, 2006, **244**, 122.
15. P. Beltrame, M. Comotti, C. Della Pina, M. Rossi, *Appl. Catal. A*, 2006, **297**, 1.
16. S. Biella, L. Prati, M. Rossi, *J. Catal.*, 2002, **206**, 242.
17. T. Ishida, N. Kinoshita, H. Okatsu, T. Akita, T. Takei, M. Haruta, *Angew. Chem.*, 2008, **120**, 9405.
18. G. Palmisano, E. García-López, G. Marcì, V. Loddo, S. Yurdakal, V. Augugliaro, L. Palmisano, *Chem. Commun.*, 2010**, 46**, 7074.
19. A. Di Paola, E. García-López, G. Marcì, L. Palmisano, *J. Hazardous Mater.*, 2012, **3-29**, 211.
20. J.C. Colmenares, R. Luque R., J.M. Campelo, F. Colmenares, Z. Karpiński, A.A. Romero, *Materials*, 2009, **2**, 2228.

21. J.C. Colmenares, A. Magdziarz, K. Kurzydlowski, J. Grzonka, O. Chernyayeva, D. Lisovytskiy, *Appl. Catal. B*, 2013, **134-135**, 136.
22. J.C. Colmenares, A. Magdziarz, A. Bielejewska, *Biores. Tech*., 2011, **102**, 11254.
23. S. Yurdakal, G. Palmisano, V. Loddo, V. Augugliaro, L. Palmisano, *J. Am. Chem. Soc.*, 2008, **130**, 1568.
24. R. Chong, J. Li, Y. Ma, B. Zhang, H. Han, C. Li, *J. Catal*., 2014, **314**, 101.
25. C. Streb, *Dalton Trans*., 2012, **41**, 1651.
26. G. Marcì, E. García-López, L. Palmisano, *Eur. J. Inorg. Chem.*, 2014, **1**, 21.
27. G. Marcì, E. García-López, L. Palmisano, D. Carriazo, C. Martin, V. Rives, *Appl. Catal. B*, 2009, **90**, 497.
28. G. Marcì, E. García-López, L. Palmisano, *Appl. Catal. A*, 2012, **421-422**, 70.
29. N. Mizuno, M. Misono, *Chem. Rev*., 1998, **98**, 199.
30. I.V. Kozhevnikov, *J. Mol. Catal. A: Chem*., 2007, **262**, 86.
31. N. Haraguchi, Y. Okaue, T. Isobe, Y. Matsuda, *Inorg. Chem*., 1994, **33**, 1015.
32. M.T. Pope, A. Müller, *Angew. Chem. Int. Ed. Engl*., 1991, **30**, 34.
33. C.R. Rocchiccioli-Deltcheff, M. Fournier, R. Franck, R. Thouvenot, *Inorg.Chem.*, 1983, **22**, 207.
34. M.S.P. Francisco, V.R. Mastelaro, *Chem. Mater*., 2002, **14**, 2514.
35. U. Lavrenčič Štangar, B. Orel, A. Régis, Ph. Colomban, *J. Sol Gel Sci. Technol.*, 1997, **8**, 965.
36. J. Tauc, *Mater. Res. Bull*., 1968, **3**, 37.
37. F. Ma, T. Shi, J. Gao, L. Chen, W. Guo, Y. Guo, S. Wang, *Colloids Surf. A*, 2012, **401**, 116.
38. Y. Roman-Leshkov, M. Moliner, J.A. Labinger, M.E. Davis, *Angew. Chem. Int. Ed*., 2010, **49**, 8954.